J Mater Sci (2006) 41:4847–4859
DOI 10.1007/s10853-006-0066-z

Strain whitening of a thermoplastic olefin material

P. Wang · I. M. Hutchings · S. J. Duncan · L. Jenkins · E. Woo

Received: 8 March 2005 / Accepted: 28 September 2005 / Published online: 4 May 2006

Abstract This paper presents research work on the characteristics and micro mechanism of strain whitening of a thermoplastic olefin material. Systematic tensile tests have been carried out to investigate the relation between strain whitening extent and external factors, including the deformation employed and the environmental temperature. A new optical method has been developed for the measurement of strain on polymer tensile samples. Applying this method relation between whitening level (grey level change) and strain has been studied. A new concept of 'strain whitening sensitivity' has been proposed and defined as the strain whitening induced by unit deformation or strain. Non-monotonic relation between whitening level and strain has been found. Strained and fractured samples were observed with A JEOL 5800 LV SEM for the micro mechanism investigation. The change of microstructure on the sample surface has been extensively observed and the combined effects of small ridges and micro-voids on the scattering efficiency of the strained surface were regarded as reasons for the non-monotonic relation between whitening level and strain.

P. Wang
Department of Materials Science and Metallurgy, University of Cambridge, Pembroke Street, Cambridge CB2 3QZ, UK

I. M. Hutchings
Institute for Manufacturing and Management, Department of Engineering, University of Cambridge, Mill Lane, Cambridge CB2 1RX, UK

S. J. Duncan
One NorthEast, Great North House, Sandyford Road, Newcastle upon Tyne NE1 8ND, UK

L. Jenkins · E. Woo
Visteon Customer and Technology Centre, Visteon UK Limited, Endeavour Drive, Basildon, Essex SS14 3WF, UK

P. Wang (✉)
Technical Department, Bridon International Ltd., Carr Hill, Doncaster DN4 8DG, UK
e-mail: wangp@bridon.com

Introduction

Thermoplastic olefins (short form TPO) are a class of materials consisting of blends of polypropylene (PP) with a rubbery phase, typically EPR (ethylene-propylene rubber) or EPDM (ethylene-propylene-diene monomer). The distinction between an impact modified PP and a TPO is arbitrary; it is suggested that PP compounds with rubber levels above about 20% can be termed TPO [1]. Since the early 1990s the short form TPO has been widely used in the automotive industry as more and more thermoplastic olefins were introduced into the automotive industry.

TPO offers several desirable advantages over other polymer materials previously used for automotive components: cost and weight savings compared with PVC/ABS [2]; acceptable heat and UV resistance [3] and corrosion resistance; complete recyclability; excellent processability for manufacturing components with complex and curved shapes, offering various styling opportunities; noise reduction, fewer squeaks and rattles, less use of anti-squeak tape; moulded-in colour to eliminate costly painting. But there are also limitations: the relatively poor scratch (mar) resistance has become an increasingly important issue which threatens TPO's application in the automotive industry [2, 4–6]. Scratches can directly cause significant repair costs. More importantly, scratch damage detracts from the subjective perception of product quality. Since

1998 authors of this paper have carried out a comprehensive research project on the scratch of TPO materials. The quantitative characterisation techniques [7–10], the mechanism of visual perceptions [11] and the effects of other parameters including crystallinity [12] have been investigated. Both analyses of scratches on real automotive components and experiments on the visual perception of simulated scratch images and laboratory-produced scratch samples have revealed that visibility of a scratch is the most important factor contributing to the subjective perception of scratch damage. Primary investigation showed that scratch visibility is caused by strain whitening and the accompanying change in colour. Straining whitening is usually called ''stress whitening'' and refers to the phenomenon that when polypropylene and other polymer materials are deformed to a certain extent, they become whiter visually, their transparency is decreased and/or reflectivity (and grey level) increased. One typical example is seen in the necked regions of polypropylene samples in tensile tests. For isotactic polypropylene, the mechanism of stress whitening is the formation of micro-voids caused by separation of crystallites parallel to the loading direction, which strongly reflect visible light and give a whitened appearance. We think it is the strain, rather than the stress that causes whitening, therefore the term 'strain whitening' is used in this paper. So it is essential to understand the phenomena and micro mechanisms of strain whitening in polymer materials, which is the objective of this paper.

This paper starts with systematic tensile tests to investigate the relation between strain whitening extent and external factors, including the deformation employed and the environmental temperature. The change of whitening extent with time after tensile extension was also investigated, in order to understand the recovery process in deformed samples. The combined effects of temperature and time on the change of grey level of deformed samples in the relaxation process are important for the accurate measurement of scratch visibility and the repairing of scratches in industrial practice.

A new concept of 'strain whitening sensitivity' is introduced and defined. In order to evaluate and compare the scratch behaviour of polymer materials, scratching tests under constant conditions (of indenter geometry, speed, temperature, and most importantly load) are usually carried out. However strain whitening results directly from micro-deformation of the polymer materials, raising the question whether under the same extent of deformation or strain different polymer materials will be whitened to the same or different extents. It is assumed that a smaller extent of whitening will lead to lower scratch visibility. An intrinsic property of a polymer material, stain whitening sensitivity, has therefore been proposed, defined as the strain whitening induced by unit deformation or strain. This proposal is explained in the present paper, image analysis is integrated with conventional tensile testing to produce an experimental system for strain whitening measurement. The correlation between whitening effect (expressed as grey level change) and strain (relative reduction of section area) is then studied for TPO material.

A detailed study of strain whitening in tensile deformation of polypropylene has been carried out by Liu and co-authors [13–15]. They proposed a mechanism, based on SEM observation of longitudinal cross-sections, but did not examine the surfaces of the drawn samples, where whitening originates, but instead examined freeze-fractured longitudinal cross-sections to represent the interior of the sample. In this paper we shall examine the microstructures both inside the materials as well as on the surface, with the aim of gaining a general understanding of the strain whitening behaviour and mechanism.

Experimental materials and methods

Experimental materials

TPO tensile bars were injection moulded by Basell UK (Grade D1194). Firstly polypropylene in the form of pellets was compounded with rubber phases, mineral fillers, and other additives to produce TPO pellets. Tensile bars with the same composition were then injection moulded by Basell with a laboratory scale injection moulder. The material flow direction was the longitudinal axe of the sample. As an example, Table 1 summarises the properties

Table 1 The properties of a typical instrument panel TPO material [16]

Property Density	Unit kg m^{-3}	Test method ISO1183	Value 1.00
Tensile yield stress	MPa	ISO527 50 mm min^{-1}	22
Flexural modulus	GPa	ISO278 2 mm min^{-1}	1.7
Izod notched impact strength at 23 °C	kJ m^{-2}	ISO180/1A	25
Izod notched impact strength at 23 °C	kJ m^{-2}	ISO180/1A	5
Heat deflection temperature HDT 1.8 Mpa	°C	ISO 75A	58
Heat deflection temperature HDT 0.45 Mpa	°C	ISO 75B	96
Coefficient of thermal expansion (parallel) 296–353 K	$\times 10^{-4}$ K^{-1}	DIN 53752	0.7
Gloss at 60°	%		2.3

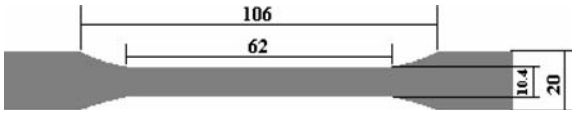

Fig. 1 The dimensions of tensile test bars in mm (thickness = 4.0 mm)

of the TPO material used in the present project [16]. The size of the sample is shown in Fig. 1. The surface roughness R_q was 0.38 μm. Colour was warm blue (Ford Motor Company colour code).

Experimental methods

A screw driven tensile testing machine (Hunsfield Test Equipment, Surrey, England, model H5K-S) was used. The maximum load capacity was 5000 N, but a load cell of capacity 1000 N with a measuring resolution of 0.1 N over the full range was used in this project; the load sampling rate was 200 Hz. Maximum extension was 600 mm with extension resolution 0.1 mm. Test (cross head) speed was between 0.001 and 1000 mm per minute (1.67×10^{-5} mm to 16.7 mm per second), and the accuracy was ±0.05 % of the set speed. Specially designed (Hunsfield) software operating in MS Windows was used for test control and measurement.

Experiments were performed at room temperature and controlled in the range of 6 °C to 32 °C to an accuracy of ±1 °C, at a constant speed of 10 mm per minute (0.17 mm s^{-1}). Samples were drawn to four pre-set extensions (25, 50, 100, 150 mm) and kept at these extensions for 10 seconds (the extension at fracture of the material was well over 300 mm). Then the load was released by decreasing the extension at the same speed of 10 mm per minute. Samples were then optically scanned to record the change of grey levels and dimensions at different times after drawing. Tensile tests and the subsequent scanning results at temperatures of 6–8 °C, 20–22 °C and 30–32 °C were analysed to explore the effects of temperature.

Grey level measurement was made with a flat bed scanner, calibrated with an optical densitometer. Details can be found at another publication of the authors [10]. Observation of surface morphology was carried out on a JEOL 5800 LV scanning electro microscopy. Methods of sample preparation is described in Section 3.5 of this paper.

Experimental results and discussions

Stress–strain characteristics of TPO

Tensile extension tests were carried out at a fixed temperature of 15 °C to gain basic information on the stress–strain characteristics of the TPO samples. Figure 2 shows a typical stress–strain curve. This TPO sample yielded at an extension of 7.0 mm (elongation 7.0/62.0 = 11%) with a yield strength of about 24.5 MPa. The sample fractured at an extension $\Delta l = 367.2$ mm or elongation = $\Delta l/l_o = 592$ % where $l_o = 62.0$ mm is the original gauge length of the tensile sample.

Recovery of TPO after deformation

The recovery process and the effects of temperature were studied by conducting tensile extensions at different temperatures and keeping the sample at zero load at the same temperature to recover. Samples were scanned at different times, and elongation and total grey level change of the gauge section were measured. Four extensions and three temperatures were chosen: 25 mm, 50 mm, 100 mm and 150 mm; and 8 °C, 20 °C and 30 °C. The relations between remaining elongation and time at three different temperatures are illustrated in Fig. 3, while that between total grey level change and time are showed in Fig. 4.

From Figs. 3 and 4 it can be seen that elongation decreased steadily with time due to relaxation, but the relation between total grey level and time was more complicated. In most cases, after an initial declining period, the grey level rose and then fell again. A related

Table 2 Remaining extensions after drawing

$\Delta l_{applied}$ mm	Δl_{0h} mm	Δl_{50h} mm	Δl_{13000h} mm	$\Delta l_{0h}/\Delta l_{applied}$	$\Delta l_{50h}/\Delta l_{applied}$	$\Delta l_{13000h}/\Delta l_{applied}$
12.00	7.18	1.5	0.9	0.60	0.13	0.08
20.00	12.70	4.2	3.8	0.64	0.21	0.19
25.00	17.52	6.7	6.5	0.70	0.27	0.26
35.00	26.00	12.2	11.2	0.74	0.35	0.32
50.00	39.38	20.7	18.3	0.79	0.41	0.37
75.00	62.08	37.7	33.5	0.83	0.50	0.45
100.00	83.88	53.5	47.0	0.84	0.54	0.47
150.00	131.00	93.0	82.2	0.87	0.62	0.55
200.00	178.00	133.2	118.7	0.89	0.67	0.59
300.00	271.20	221.0	203.0	0.90	0.74	0.68

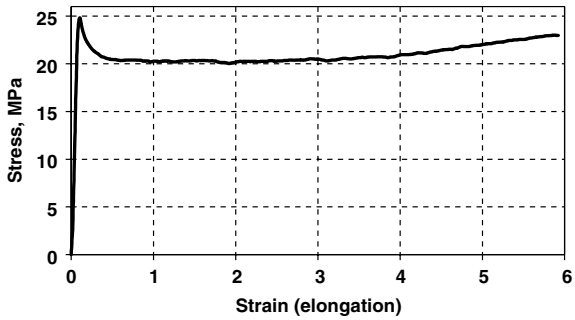

Fig. 2 Typical stress–strain curve of TPO (at 15.0 °C); sample fractured at an extension of 367.2 mm, corresponding to an engineering strain of 5.92

phenomenon was also observed on a single tensile sample, as described in the following section; the mechanism responsible will be discussed in Section 3.5

The effects of temperature are complicated. Increasing temperature can enhance the plasticity of the polymer in tensile deformation to produce higher initial elongation. It also boosts the recovery after deformation, which reduces the residual elongation. From Fig. 4 it can be seen that for the same initial extensions, deformation at lower temperature produced greater strain whitening. This is probably because more deformation features such as crazes were generated at lower temperature in order to achieve the extension. After the initial extension, the recovery depended more on temperature; at lower temperature the mobility of polymer molecules was lower than at higher temperature, so that surface features were remained. So the higher total grey level in samples strained at lower temperatures retained during the recovery process. It should also be pointed out that 8 to 30 °C is only a small range of temperature between the glass transition temperature (well below −10 °C) and melting point (~180 °C) of polypropylene.

A new method of strain measurement

The fact that strain in a tensile sample of TPO was found to be inhomogeneous, varying along the gauge length of the specimen, allowed the dependence of grey level on strain to be measured for individual tensile samples. The value of the grey level of each pixel can be measured by using the optical scanning technique described in another publication [10]. Strain can be determined optically. Two scanning and

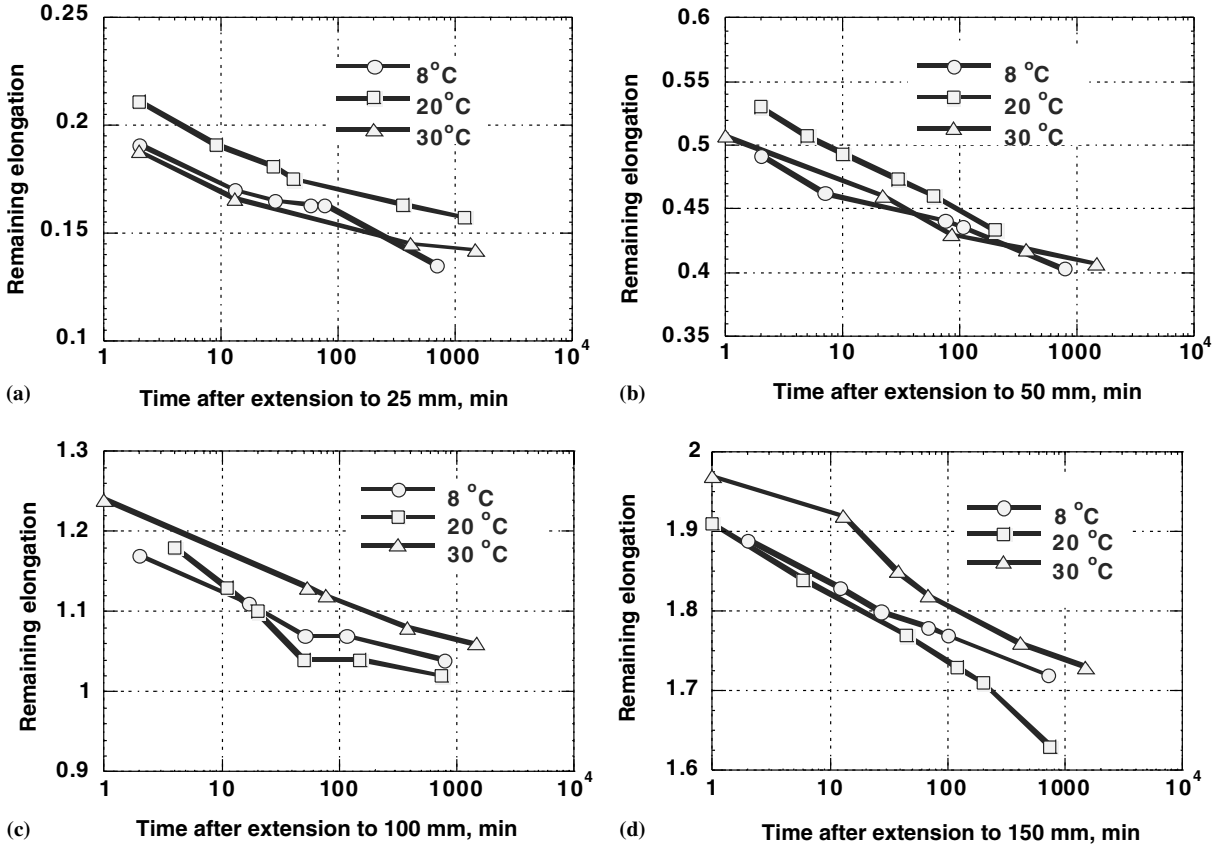

Fig. 3 Relation between remaining elongation and time at three different temperatures. Initial extensions in (**a**), (**b**), (**c**), (**d**) are 25 mm, 50 mm, 100 mm and 150 mm respectively

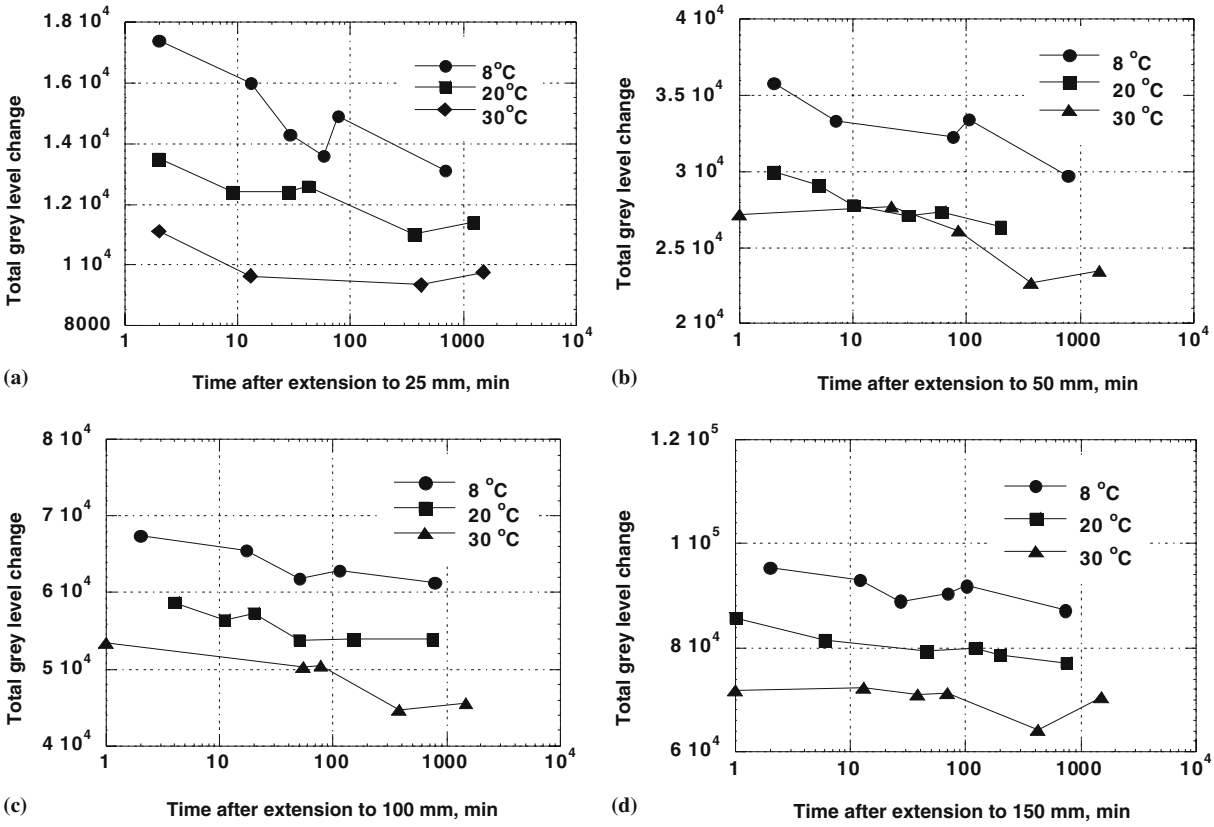

Fig. 4 Relation between total grey level change and time at three different temperatures. Initial extensions in (**a**), (**b**), (**c**), (**d**) are 25 mm, 50 mm, 100 mm and 150 mm respectively

image processing methods were tested for the recording and measurement of sample dimensions: transmissive scanning and reflective scanning. For scanners with transmissive scanning accessories the operation was simple: place the sample flat on the scanner bed and scan in transmissive mode to record sample width and in reflective mode to record grey level. Sample thickness can be measured by scanning a sample placed vertically in transmissive mode. In this way at each point along the gauge length of the tensile sample the strain, relative reduction in section area as expressed in equation (1), and the corresponding grey level change can be obtained.

$$\varepsilon = \frac{\Delta A}{A_o} = \frac{A_o - A}{A_o} = 1 - \frac{A}{A_o} = 1 - \frac{wh}{w_o h_o} \qquad (1)$$

where ε is the strain; A is the section area and A_o is the original section area; w is the width and w_o is the original width; h is the thickness and h_o is the original thickness.

Thus a grey level change versus strain relation with high spatial resolution (for scanning resolution 600 dpi, the size of a pixel is 0.042 by 0.042 mm) is available. The accuracy of dimensional measurement by optical scanning was confirmed by comparing the measurement results with a screw micrometer (accuracy 0.002 mm) and with the scanning method. The samples were 0.5 mm thick, 10 mm wide steel sheets with several lengths between 2 mm and 10 mm. It was found that the difference between the two methods was less than 0.02 mm. Now scanners with optical resolution of 2400 dpi are commercially available, for which the size of a pixel is 0.01 mm.

For scanners without transmissive mode the standard procedures described in [10] were used to scan samples placed flat on the scanner bed in reflective mode. For above experimental results, we can derive:

- Total grey level change at a given extension;
- The value of grey level, width and thickness at each point along the gauge section of a drawn sample;
- Strain and grey level change vs strain curves: $\Delta G \sim \varepsilon$.

Figures 5 and 6 showed an example of the above process. The grey level change $\Delta G \sim \varepsilon$ curve can be defined as the 'whitening sensitivity' curve. As discussed earlier in paper, this curve provides important information about the property of the material which influences the visual effects of scratches made on the surface.

Fig. 5 The measurement of width (**a**, **b**, **c**) and grey level along sample gauge length. The image was scanned at 2nd minute after the sample had been drawn to extension 50 mm

(a) The image of the gauge section of a deformed sample. The image was scanned at 2nd minute after sample was drawn to an extension of 50 mm at 15°C. The width at the right end is 10.4 mm.

(b) A new image for width calculation, formed by filling the above image with 100% black. The width at the right end is 10.4 mm.

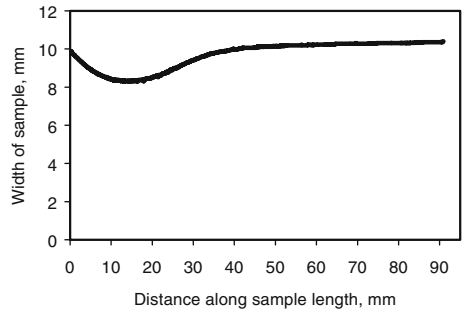

(c) The change of width along sample length deduced from the plot profile of grey level change.

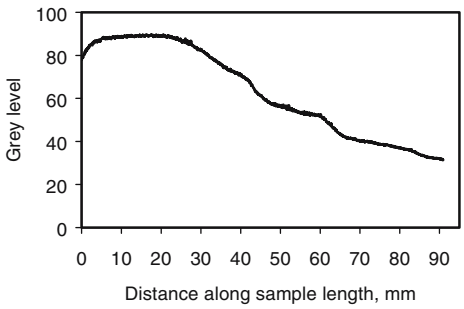

(d) The change of grey level along the gauge length of sample.

Relation between strain and grey level change

The method of optical scanning allowed both the strain and grey level change to be measured at a particular point along the gauge section of a tensile sample. The relation between grey level change and strain could then be studied. Figure 7 shows the measurements of strain and grey level change for tensile samples that were drawn to the four initial extensions (25, 50, 100, 150 mm) at 8 °C, during relaxation at various times after straining.

Tensile tests with polymers including polypropylene have shown that after yielding occurs a neck with constant dimension is formed and develops along the gauge length until the whole specimen is necked [17]. For TPO the deformation did not localise to form a distinct neck, but instead changed more gradually and continuously along the gauge length. The reason is probably that the addition of

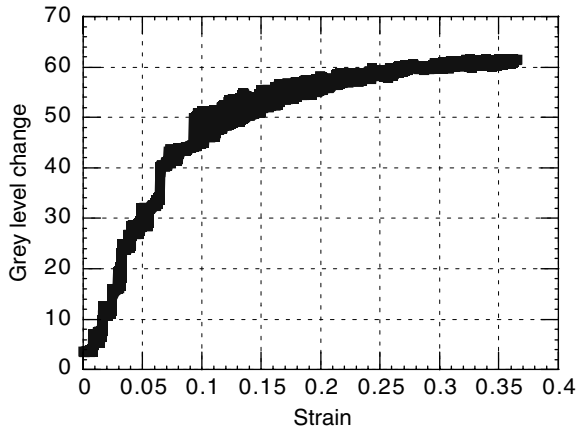

Fig. 6 Grey level change (ΔG) vs strain (ε) curve for the example shown in Fig. 7

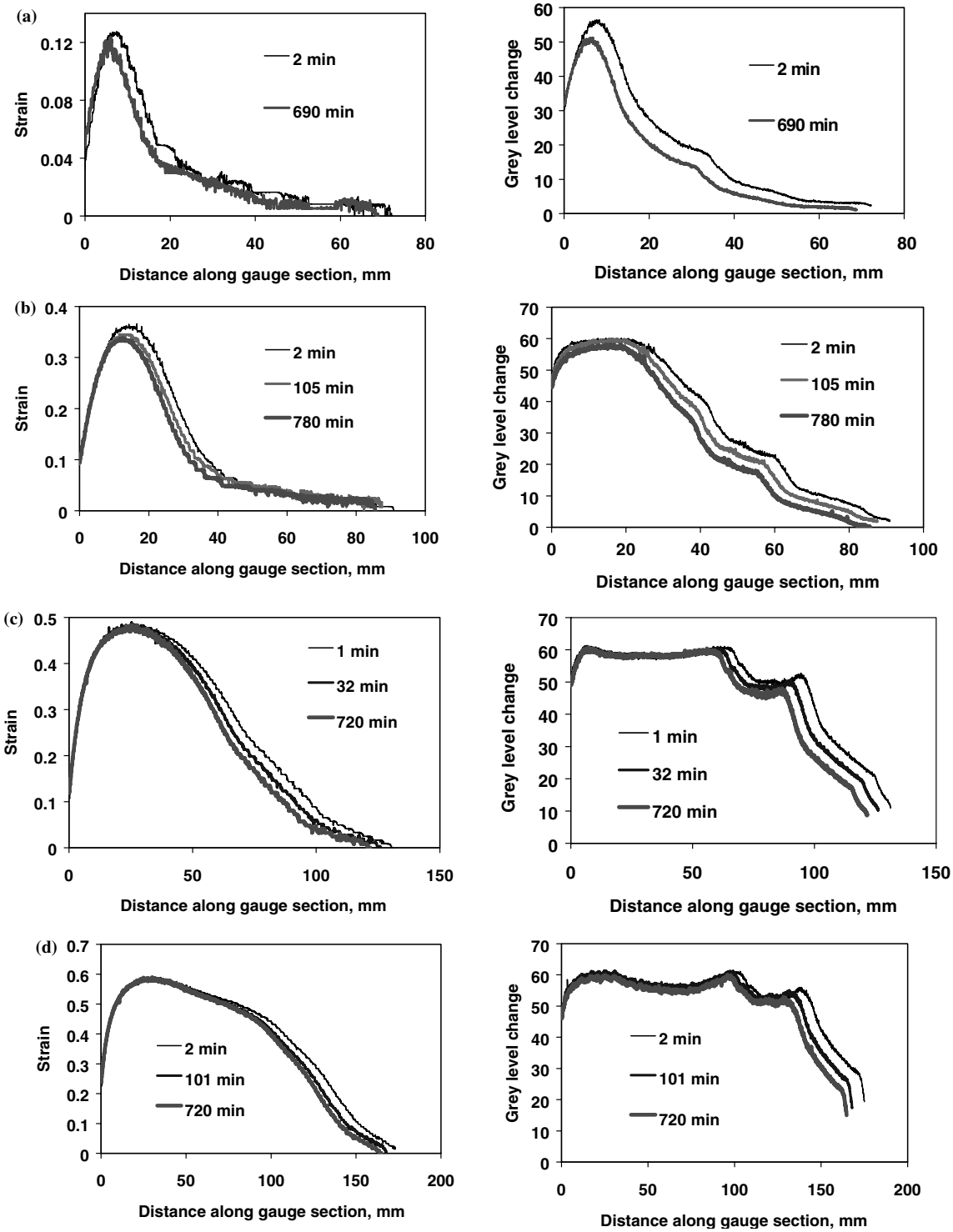

Fig. 7 Strain and grey level change along gauge distance on four samples with initial extensions being 25 mm (**a**), 50 mm (**b**), 100 mm (**c**) and 150 mm (**d**)

the ethylene-propylene rubber particles, and of mineral fillers restricted the extent of strain hardening. Figure 7 shows that after each extension the tensile sample recovered with time, i.e. both strain and grey level change decreased with time. Though there are some overlapping and complex cases at some places on the gauge length, the general trend is of steady recovery in all parts of the gauge section.

While the strain decreases along the gauge length, the grey level change on samples with initial extension 100

and 150 mm was not monotonic, i.e. the grey level change at a smaller strain was higher than that at a bigger strain. The data shown in Fig. 7 were replotted to show grey level change verses strain, as shown in Fig. 8. Then it can be seen that for the same sample at the same strain, grey level change was higher at the early stage of recovery (after 1–2 min), but decreased a little at longer times (e.g. 720 min). The non-monotonic relationship between grey level change and strain can be seen on samples with larger initial extensions (100 and 150 mm). For the sample with 150 mm initial extension, the grey level at a strain of 0.42 was higher than that at a strain of 0.50. This brings about potential problems for precise measurement of grey level changes caused by scratches and the visibility of scratches. The mechanism is discussed in following sections. It can also be seen that for the same strain, values of grey level changes at the early stage of recovery (e.g. 2 min) were almost the same as those at longer times (e.g. 720 min). Grey level changes verses strain curves for the same recovery time (2 min after extension) have been superimposed for the four samples with different initial extensions, as shown in Fig. 9. It can be seen that values of grey level changes of the four samples are close to each other, especially in small strain region (less than 0.2). Nevertheless the initial elongation should be specified when tensile tests are carried out to measure strain whitening sensitivity.

Mechanisms of strain whitening

Preparation of SEM samples

Tensile samples were drawn to fracture at 10 mm min^{-1} and 15 °C. For SEM observation on surfaces the samples were sputter coated with gold to increase electrical conductivity. For SEM observation of the internal microstructures, the samples were freeze-fractured along the longitudinal central line in liquid nitrogen. A JEOL 5800 LV scanning electron microscope was used with an acceleration voltage of 10 kV and secondary electron imaging. The change of surface morphology with strain was examined to investigate the micro mechanism of strain whitening and its variation with tensile extension.

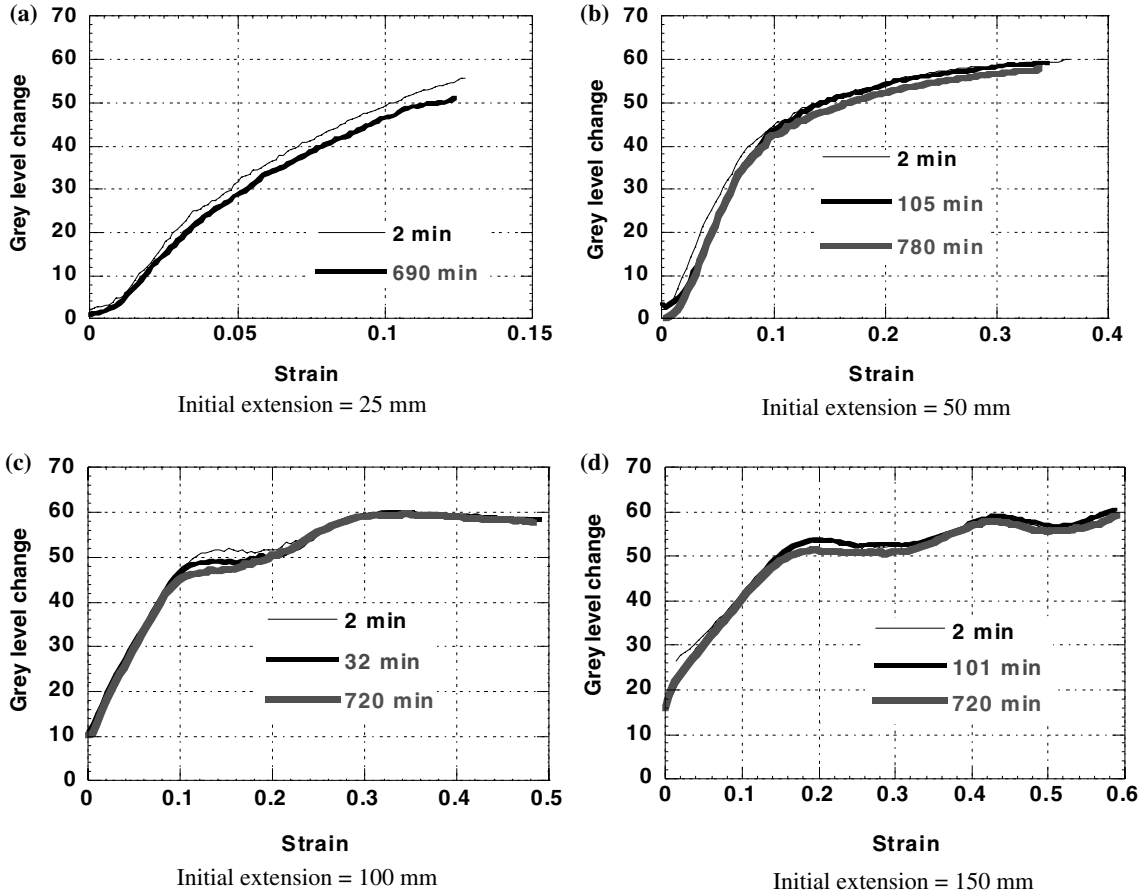

Fig. 8 Relation between grey level change and strain on four samples with initial extension being 25 mm (**a**), 50 mm (**b**), 100 mm (**c**) and 150 mm (**d**)

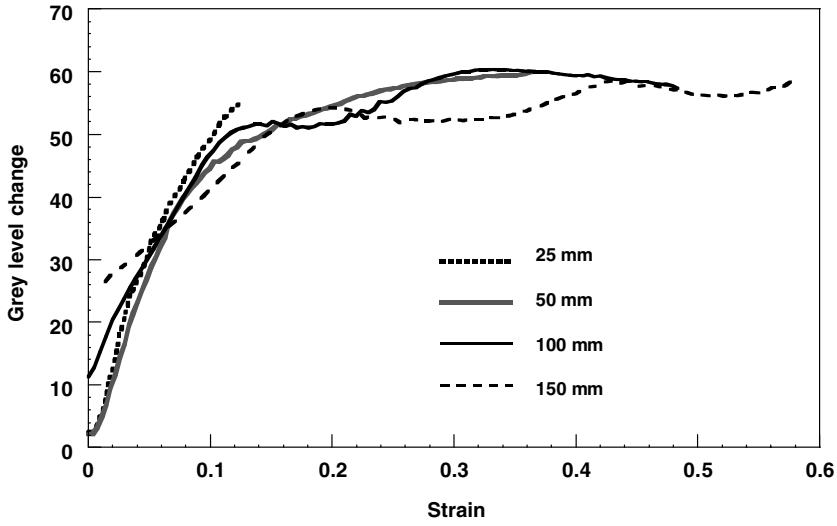

Fig. 9 Relation between grey level change and strain measured at the same time (2 min) after tensile tests for the four samples with different initial extensions 25, 50, 100 and 150 mm

Change of morphology with strain

At small strain ~2% a number of rib-like deformation marks appeared on the sample. When strain increased to about 10% the sample yielded and a grey level change was visually noticeable. On the surface locally broken areas began to appear, Fig. 10 (a), followed by small ridges lying perpendicularly to the tensile direction at a strain between 10% and 30%, (b) and (c). At around 50% strain the sample was thoroughly whitened and severely deformed fibrils were the dominant features on the surface, Fig. 10 (d). At this stage no small ridges was observed.

These SEM observations show the general process by which the surface morphology changed with increasing strain. At higher strain the microstructures of the sample became very porous, consisting of severely deformed fibrils and voids between them. This is similar to the microstructure inside a craze, which has been well studied. But the mechanism of the formation of the small ridges needs more detailed study. Whether formation of the small

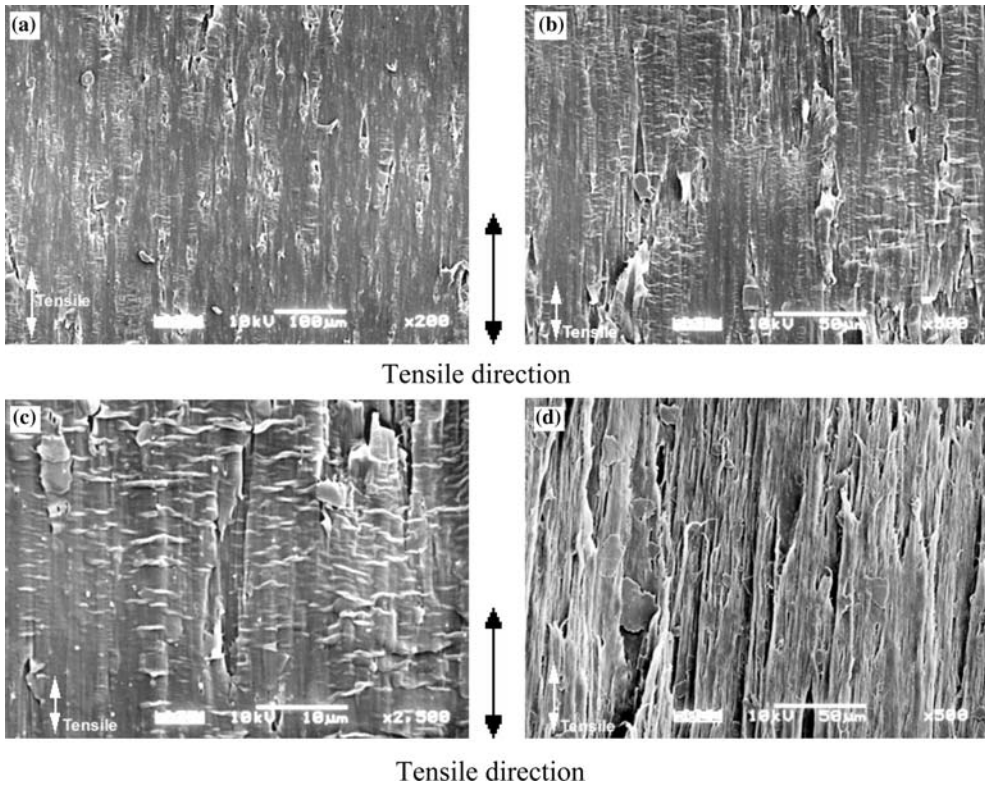

Fig. 10 Change of surface morphology with strain increasing until sample fracture. (**a**): strain about 10%—some areas were locally broken; (**b**, **c**): strain about 30%—small ridges developed lying perpendicularly to tensile direction; (**d**): near fracture surface, strain about 50%—material severely deformed and transformed into fibrils, mineral particles detached

ridges is related to the non-monotonic relation between grey level and strain is of great interest as is the role of mineral fillers.

Micro mechanisms

Figure 11 (a) shows a general view of the broken area, with some small ridges lying perpendicular to the tensile direction. Figure 11 (b) shows an area at higher magnification, and reveals that the small ridges were wrinkles of polymer matrix. The curled edge marked 'C' was the result of further relaxation when the polymer layer marked 'B' broke up from position 'A'. This and other images confirmed that the small ridges were wrinkles of polymer formed when the stress was released. Image (c) was taken at a location with higher strain; more ridges were captured (the lower right part of the image) and at the same time at other areas small holes began to appear (shown by arrows) as a result of the separation of the polymer material. At higher strain the ridges were separated into sections due to separation of the polymer matrix perpendicular to the tensile direction, and with strain intensifying the ridges were stretched to become straight and eventually the ridges disappeared and transformed into fibrils. Image (d) of Fig. 11 shows how the previous ridge A1–B1–C1 was sectioned into three parts and stretched straight.

Figure 12 shows SEM images of the microstructures in the most severely deformed area near the fracture location. (a) show the effects of the mineral particles on the plastic deformation of the polymer matrix. Mineral particles reduced the capacity for plastic deformation of the polymer matrix, which increases the intensity of polymer deformation and increases whitening. (b) shows the formation of micro voids. Details of a stress–strain curve of TPO exhibited the quasi periodic build-up and release of stress in the extension process after yielding, Fig. 13. This is consistent with the explanation of the formation mechanism for the small ridges discussed above. The number of small ridges is much higher than that of the steps on the tensile curve, and each drop in stress resulted from the collective contributions of many ridges.

Ridges and non-monotonic relation between grey level and strain

The above study reveals the nature of the small ridges on the surfaces of strained TPO samples. But direct observation of their interaction with incident light is not easy, as small ridges and stretch marks often appear on the surface at the same time. The size (width) of the ridges was often similar to the wavelength of visible light. So theoretically they should enhance the scattering efficiency of the surface.

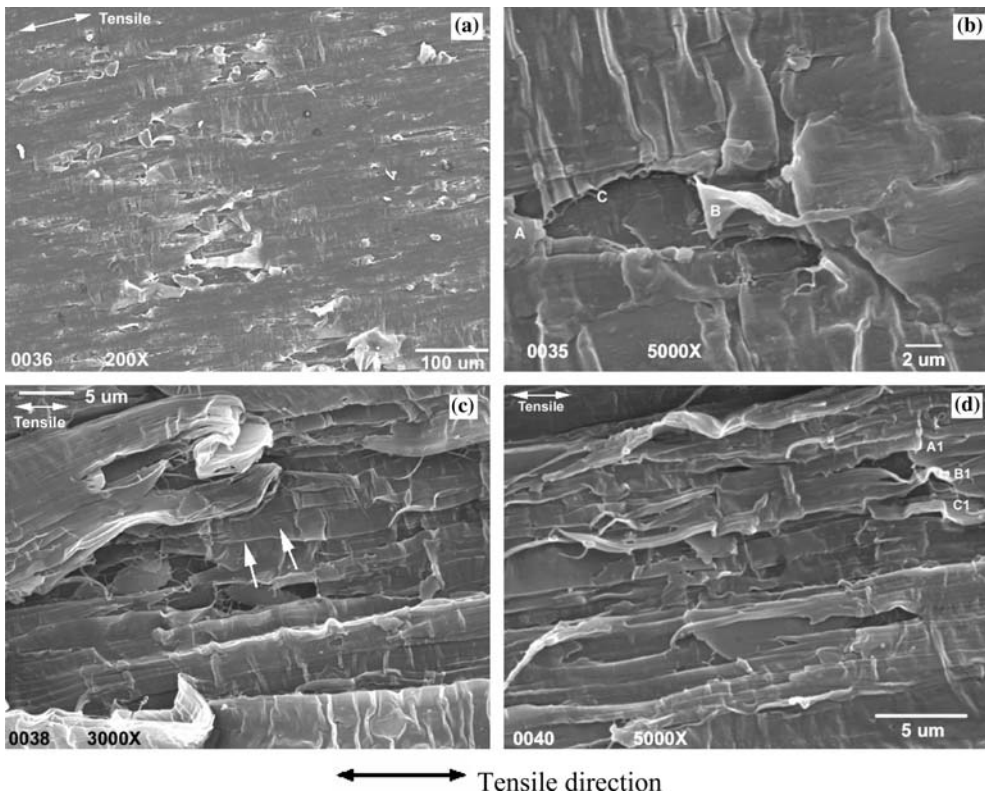

Fig. 11 SEM images of a tensile strained and broken sample. (**a**) shows a general view of the area where surface began to break up locally with strain being about 10%; (**b**) shows a pit from (**a**) at a higher magnification: a stretched layer marked with the letter 'B' broke up at a surface irregularity 'A', released local stress and left curled edge 'C'; (**c**) was taken at a place with strain around 30% — more wrinkle like ridges can be seen (lower right in the image), very small elliptic voids are marked with two arrows indicating the separation of the polymer matrix; (**d**) shows that at higher strain (50%) a ridge that had existed along 'A1', 'B1', 'C1' was separated into three sections A1, B1, C1 and then stretched straight

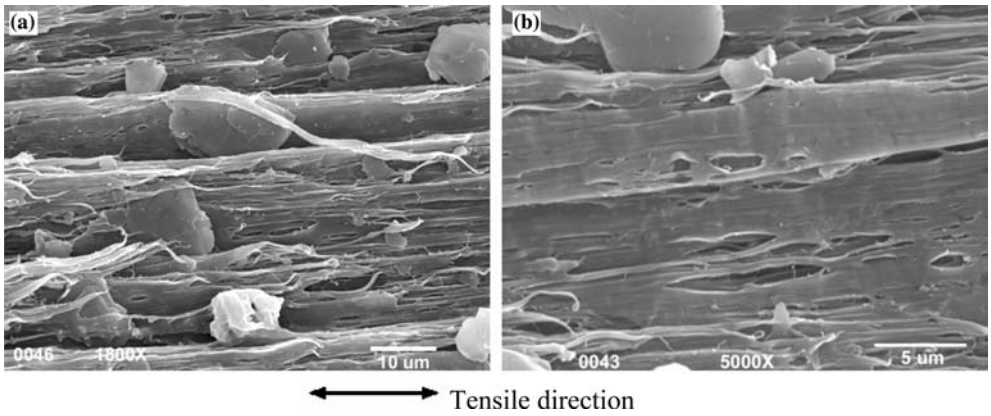

Fig. 12 SEM images of the surface features in the most severely deformed area near the fracture surface with strain above 50%. (**a**) Shows the effects of mineral particles on the plastic deformation of polymer matrix; (**b**) exhibits the formation of micro voids

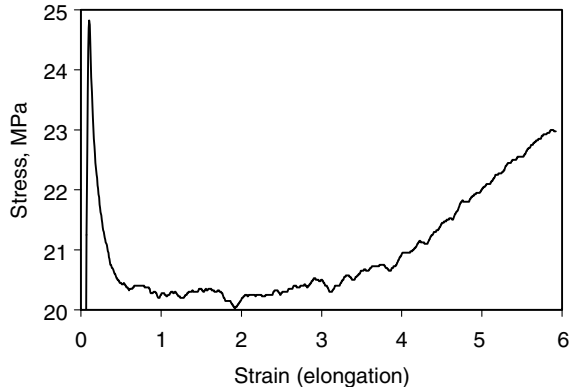

Fig. 13 Details of stress–strain curves after yielding, part of the tensile extension process shown in Fig. 2. The irregularities on the curve correspond to the formation of small ridges on surfaces of tensile samples. This TPO sample was extended at strain rate of 10 mm min^{-1} and yielded at an extension of 7.0 mm (elongation 7.0/62.0 = 11%) with a yield strength of about 24.5 MPa. The sample fractured at an extension Δl = 367.2 mm or elongation = $\Delta l/l_o$ = 592% where l_o = 62.0 mm is the original gauge length of the tensile sample. Ambient temperature was 15 °C

Ridges appeared with increasing strain yet disappeared on further strain. This produced a very similar hilly relationship between scattering and strain to that between scattering efficiency and particle size of whitening pigments [18]: there existed an optimum size (close to the half wavelength of green light) of pigments, at which highest scattering efficiency was generated.

Size and concentration of micro-voids and the non-monotonic relation

Besides the effects of small ridges, the contribution to light scattering from fibrils and micro-voids in crazes of further deformed polymer should also be discussed. It should be noticed that when deformation intensifies, not only the total number of micro-voids but also the size and shape of the micro-voids will be changed.

Research on the mechanism of crazes shows that the subsequent growth occurs not by repeated nucleation of new voids but by a process in which the existing voids advance finger-like extensions into the bulk polymer, eventually linking up and leaving stretched fibrils in their wake [17]. Besides the main fibrils that lie vertically to the general orientation of a craze and bridge the two surfaces, there are also cross-tie fibrils which link up the main fibrils, observed by electron diffraction and transmission electron micrographs. So the non-monotonic relation is probably also related to the combined and complex effects of size and concentration of micro voids on the light scattering. At the early stage of deformation, the contribution to scattering by concentration increases with strain as more and more micro voids are produced. If we define concentration as the number of scattering centres in a unit surface area, any growth of micro voids will decrease concentration and thus scattering efficiency. The variation of the contribution of size poses a trend similar to those of pigments when strain increases the size of micro voids [19]. Because the most efficient scattering occurs at different strain values, the combined effect has periodic variations, as shown in Fig. 14. There exist other factors that may influence light scattering, such as the change in refractive indices caused by molecular scale changes such as reorientation and entanglement of polymer molecules, the change of shape of the craze and its sub structures, as well as other components in the polymer material, such as rubber particles and mineral fillers. Strain whitening is a complicated phenomenon with a number of mechanisms operating often at the same time and strain. Further research is necessary to confirm the proposed mechanisms.

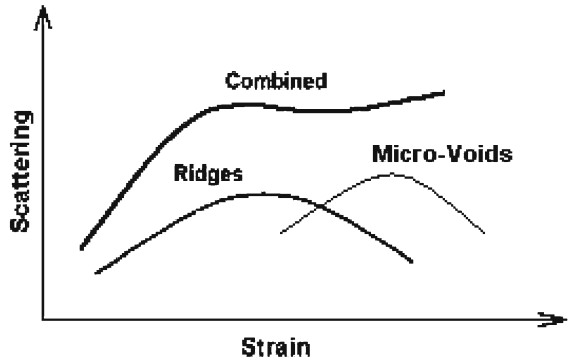

Fig. 14 Model for the effects of ridges and micro-voids on light scattering efficiency and the non-monotonic relation between grey level and strain

Conclusions

Strain and whitening characteristics of TPO upon tensile deformation

1. Tensile tests showed that the higher the initial tensile extension applied to TPO, the larger was the residual extension. This is because elastic deformation accounts for a greater proportion of smaller extensions than of larger extensions. The higher the applied extension the higher was the total grey level change on the sample: this relationship also applied for residual extension and total grey level change at all times after drawing.
2. Over the range of temperature used (8–30 °C), no simple relation was found between residual elongation and temperature. But it was found that higher total grey level change was generated at lower temperatures.
3. A new method, based on tensile testing and image acquisition and analysis, has been developed for the measurement of both grey level and strain. Grey level change versus strain curves were derived. A new property of polymer materials, strain whitening sensitivity, was proposed and defined as grey level change per unit strain. Grey level change—strain curves provide important information about the whitening of a polymer material.
4. A non-monotonic relationship was found in the grey level change versus strain curves, i.e. in some cases higher strains generated lower grey level changes. This together with the non-monotonic relation in total grey level change - recovery time curves can affect the accurate measurement of strain whitening, because it means that in scratch visibility tests it is possible to get a lower value of grey level change at a higher applied load. The reason for this phenomenon was investigated together with the strain whitening process and mechanism in the TPO material.

Strain whitening process and mechanism in TPO

(1) At the beginning of tensile extension (strain of section reduction 2%), a number of long-rib like deformation marks appeared on the sample with grey level slightly higher than the original surface. Within these ribs are deformation lips lying at about 45° to the tensile direction. When strain increased to about 10% the sample yielded and a grey level change was visible. On the surface, pits began to appear, followed by small ridges lying perpendicularly to tensile direction at a strain of 10–30%. At higher strain (>30–50%) the sample was thoroughly whitened and severely deformed fibrils were the dominant features on the surface. At this stage, few small ridges were observed. At higher strain the microstructures of the sample became very porous, consisting of severely deformed fibrils and voids between them. This is similar to the microstructure inside a craze, which has been well studied. Comparing with the microstructures of polypropylene, it can be seen that the presence of rubber particles and mineral fillers made the material much more porous after deformation.

(2) SEM observation revealed the small ridges to be wrinkles of polymer surface formed when stress was released. Steps on the stress–strain curves of TPO showed the quasi-periodic build-up and release of stress in the extension process after yielding. Each drop in stress resulted from the collective contributions of many ridges.

(3) The reason for the non-monotonic relation between grey level and strain. It is suggested that formation of the small ridges is related to the non-monotonic relation between grey level and strain. The fact that ridges developed and then disappeared with increasing strain produced a very similar relation between scattering efficiency and strain to that between scattering efficiency and particle size. The other possibility is the combined and complex effects of the size and concentration of micro voids on light scattering. However whitening is a complicated phenomenon with a number of mechanisms operating often at the same time and strain. Further research is necessary to confirm the proposed model.

References

1. Moore EP Jr (1996) In: Polypropylene handbook, Hanser Publishers
2. Sanford W, Dawson R, Deanr D (1998) In: Proceedings of the Fifth International Conference on TPOs in Automotive'98, 12–14 October 1998, Michigan, USA

3. Exxon Company (information leaflets), the Fifth International Conference on TPOs in Automotive'98, 12–14 October 1998, Michigan, USA
4. Florence R, Sherman K (1997) Automotive Eng 105(5):39
5. Chu J (1998) In: Proceedings of International SAMPE Symposium and Exhibition, vol. 43, No. 2, 1998, p 1149–1157, ISSN: 0891–0138 CODEN: ISSEEG. Conference: Proceedings of the 1998 43rd International SAMPE Symposium and Exhibition. Part 2 (of 2), May 31–Jun 4 1998, Anaheim, CA, USA
6. Chu J, Rumao L, Coleman B (1998) Polym Eng Sci 38(11):1906
7. Wang P, Hutchings IM, Duncan SJ, Jenkins L, SAE Technical paper Series, 1999–01-0243; also published in SAE Transactions, Journal of Materials and Manufacturing, 108 (1999) 134
8. Wang P, Hutchings IM Duncan SJ, Jenkins L (1999) In: Proceedings of the 6th International Conference on TPO in Automotive, October 25–27, 1999, Novi, Michigan, USA
9. Wang P, Hutchings IM, Duncan SJ, Jenkins L, Woo E (2000) In: Proceedings of SPE Automotive TPO Global Conference 2000, October 2–4, 2000, Dearborn, Michigan, USA, pp 107–119
10. Hutchings IM, Wang P, Parry GC (2003) Surf Coat Tech 165:186
11. Wang PZ, Hutchings IM, Duncan SJ, Jenkins L, Woo E (2000) In: Proceedings of the 7th International Conference on TPO in Automotive, October 23–25, 2000, Novi, Michigan, USA
12. Wang PZ, Hutchings IM, Duncan SJ, Jenkins L (2001) In: Proceedings of SPE Automotive TPO Global Conference 2001, October 1–3, 2001, Dearborn, Michigan, USA
13. Liu Y, Truss RW (1995) J Polym Sci Pol Phys 33(5):813
14. Liu Y, Kennard CHL, Truss RW, Calos NJ (1997) Polymer 38(11):2797
15. Liu Y, Truss RW (1994) J Polym Sci Pol Phys 32:2037
16. Duncan S (1998) In: Proceedings of the Fifth International Conference on TPOs in Automotive'98, October 12–14, 1998, Michigan, USA
17. Young RJ, Lovell PA (1991) Introduction to polymers, 2nd edn. Chapman and Hall
18. Mascia L (1974) The role of additives in plastics, Edward Arnald (Publishers) Ltd
19. Clark DT, Feast WJ (1978) Polymer surface, John Wiley and Sons